OPTOELECTRONICS AND ADVANCED MATERIALS – RAPID COMMUNICATIONS Vol. 4, No. 6, June 2010, p. 859 - 862

Frequency dependent electrical characteristics of (Ni/Au)/AlGaN/AlN/GaN heterostructures

İ. TAŞÇIOĞLU, H. USLU, Y. ŞAFAK, E. ÖZBAY[a]
Physics Department, Faculty of Arts and Sciences, Gazi University, 06500, Teknikokullar, Ankara, Turkey
[a]Nanotechnology Research Center, Department of Physics, Bilkent University, 06800 Ankara, Turkey

The main electrical parameters such as ideality factor (n), zero bias barrier height ($_{Bo}$), series resistances (R_s), depletion layer width (W_D) and interface state densities (N_{SS}) of (Ni/Au)/AlGaN/AlN/GaN heterostructures have been extracted from the current-voltage (I-V) at room temperature, and frequency dependent capacitance voltage (C-V) and conductance-voltage (G/w-V) measurements. The high value of n and R_s were attributed to the existence of an interfacial layer (IL) and particular distribution of N_{ss}. The density distrubition profile of N_{ss} was obtained from both forward bias I-V data and low-high frequency (C_{LF}-C_{HF}) measurement methods. In addition, the voltage dependent R_s profile obtained both I-V and admittance measurements are in good agreement. As a result, the existence of an IL, R_s and N_{ss} lead to deviation from the ideal case of these heterostructures.

(Received March 01, 2010; accepted June 16, 2010)

Keywords: (Ni/Au)/AlGaN/AlN/GaN, C-V-f and G/w-V-f measurements, Interface states, Rs

1. Introduction

In the ideal case, the C and G/w of metal-insulator-semiconductor (MIS) structures is usually frequency independent but in the applications situation is different especially at low frequencies [1-4]. The interface quality at M/S interface and R_s of device decide the performance and reliability of these devices. Using a thin film between the metal and semiconductor, such as Si_3N_4, cannot only prevent the reaction and inter-diffusion between the metal and AlGaN barrier layer, but can also further improve the retention properties [5,6].In order to determine the N_{ss}, there are a lot of methods such as the I-V [7,8] and C_{LF}-C_{HF} [1,9] and quasi-static capacitance [10]. Among them, the I-V and C_{LF}-C_{HF} methods are both simple and sufficiently reliable. Therefore, in this study, to achieve a better understand the effect of R_s and N_{ss} on main electrical characteristics, we used I-V, C-V and G/w-V characteristics in the wide frequency range of 2 kHz-2 MHz.

2. Experimental procedure

The (Ni/Au)/AlGaN/AlN/GaN heterostructures were fabricated on (0001) on a double-polished 2-inch diameter (0001), in which sapphire (Al_2O_3) substrates were grown in a low pressure Metal - Organic Chemical - Vapor Deposition (MOCVD). Al_2O_3 substrate was annealed at 1100 °C for 10 min in order to remove surface contamination. The buffer structures consisted of a 15 nm thick, low-temperature (650 °C) AlN nucleation layer, and high temperature (1150 °C) 420 nm AlN templates. A 1.5 μm nominally undoped GaN layer was grown on an AlN template layer at 1050 °C, followed by a 2 nm thick high temperature AlN (1150 °C) barrier layer. The ohmic contacts were formed as a square van de Pauw shape and the Schottky contacts formed as 1 mm diameter circular dots. Then, Schottky contacts were formed by Ni/Au (40/80 nm) evaporation. The schematic diagram of (Ni-Au)/AlGaN/AlN/GaN heterostructures can be seen in our previous study [11]. The I-V and admittance (C-V and G/w-V) measurements of the (Ni/Au)/AlGaN/AlN/GaN heterostructures were performed using a Keithley 2420 programmable constant current source and an HP4192 A LF impedance analyzer in the frequency range of 2 kHz-2 MHz at room temperature.

3. Results and discussion

The forward and reverse bias *I-V* characteristics of the (Ni/Au)/AlGaN/AlN/GaN heterostructures with 40 Å insulator layer thicknesses (SiN_x) were investigated based on thermionic emission (TE) theory at room temperature. According to TE , the relationship between the I and V through a barrier, with series resistance, is given by [12]

$$I = \underbrace{AA^{*}T^{2}\exp\left(-\frac{q\Phi_{Bo}}{kT}\right)}_{I_0}\exp\left(\frac{q(V-IR_s)}{nkT}\right)\left[1-\exp\left(\frac{-q(V-IR_s)}{kT}\right)\right] \quad (1)$$

where Φ_{B0} is the zero-bias barrier height, A is the rectifier contact area, A^{*} is the effective Richardson constant and is equal to 32,09 A/cm^{2}K^2 for undoped Al$_{0,22}$In$_{0,78}$N [11], in which I_0 is the reverse saturation current derived from the straight line intercept of *lnI* at zero bias voltage. The term IR_s is the voltage drop across the R$_s$. Fig.1, shows the *lnI-V* characteristics and it shows a linear behavior. The values of I_0 and n were obtained by extrapolating and the slope of linear part of *lnI-V* plot as 6x10^{-6} A and 5.49, respectively. Φ_{B0} value was obtained from the values of I$_0$ and of rectifier contact area as 0,55 eV. This high value of n shows that the structures follow an MIS configuration rather than MS SBDs and *n* can especially be attributed to the existence of an insulator layer, a wide distribution of low BH patches, a tunneling mechanism, and the particular distribution of N_{ss} at the M/S interface [2,7,8,12,13]. It can be seen from Fig 1, the reverse current increases with the increase of the applied reverse bias and does not go to saturation especially for the reference sample. This lack of saturation for the Schottky contact on an (Ni/Au)/AlGaN/AlN/GaN heterostructure under reverse bias can be explained in terms of the spatial inhomogeneity of BH and the image force lowering in the barrier height [13]. In addition, the voltage dependent R$_s$ profile was obtained from Ohm's law ($R_i=\delta V_i/\delta I_i$) and is given in Fig1 and it has 203 Ω at 8 V.

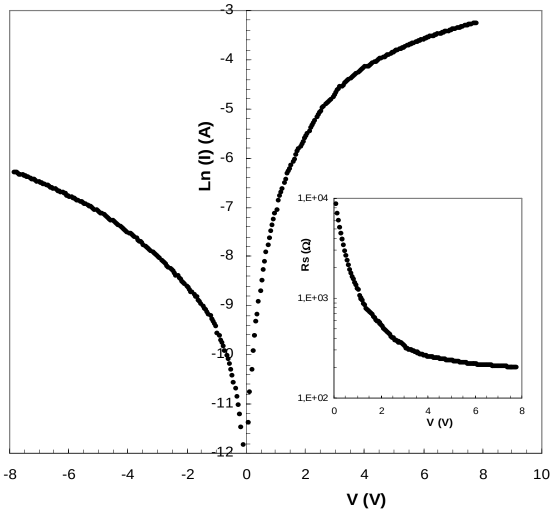

Fig. 1. The semi-logarithmic LnI-V characteristics of the (Ni/Au)/AlGaN/GaN heterostructure.

The voltage dependent *n* and effective barrier height (Φ_e) can be expressed as [8,12]

$$n(V)=\frac{qV}{kT\ln(I/I_0)} \tag{2.a}$$

$$\Phi_e=\Phi_{bo}+\beta V=\Phi_{Bo}+\left(\frac{d\Phi_e}{dV}\right)V \tag{2 b}$$

where $d\Phi_e/dV$ is the change in the barrier with bias voltage. For the MIS type structure, the expression for the N$_{ss}$ as deduced by Card and Rhoderick [8] is reduced as

$$N_{SS}=\frac{1}{q}\left[\frac{\varepsilon_i}{\delta}(n-1)-\frac{\varepsilon_s}{W_D}\right] \tag{3}$$

where δ is the thickness of insulator layer, and W_D is the depletion layer width that is being deduced from the C^{-2}-V measurements at 1 MHz. For n-type semiconductor, the energy of interface states E_{ss} with respect to the conductance band edge is given by [21-30-32]

$$E_c-E_{ss}=q(\varphi_e-V) \tag{4}$$

The energy distribution of the N_{ss} for (Ni/Au)/AlGaN/AlN/GaN heterostructures was obtained from the experimental forward bias *I-V* and is shown in Fig. 2. As can be seen in Fig. 2, the value of N_{ss} is a slight exponential increase in from the mid-gap towards the bottom of the Ec.

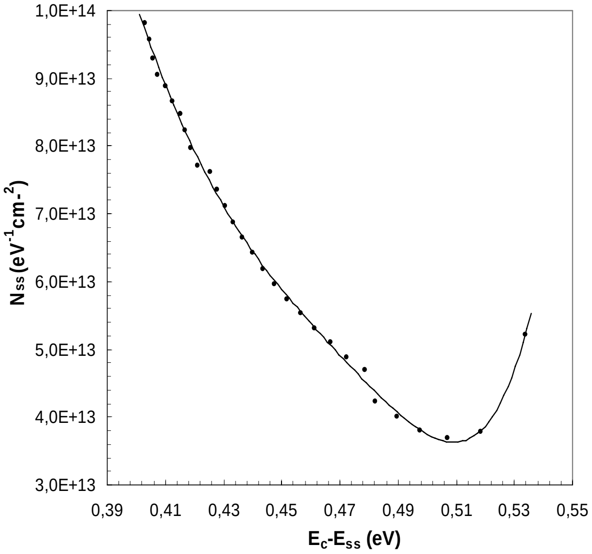

Fig. 2. The N_{ss} profile deduced from I-V data of the (Ni/Au)/AlGaN/GaN heterostructure.

The analysis of the *C-V* and *G/w-V* measurements of the high electron mobility transistors (HEMTs) only at one or narrow frequency and bias voltage range can not give us detailed information about conduction mechanisms, barrier formation, N$_{ss}$. In contrary to, in the wide frequency and bias voltage region, the *C-V* and *G/w-V* measurements of these devices can allow us to understand different aspects of conduction mechanisms. Therefore, the *C-V-f* and *G/w-V-f* characteristics of (Ni/Au)/AlGaN/AlN/GaN heterostructure have been investigated in the wide frequency range of 2 kHz-2 MHz are given in Fig. 3 (a) and (b), respectively.

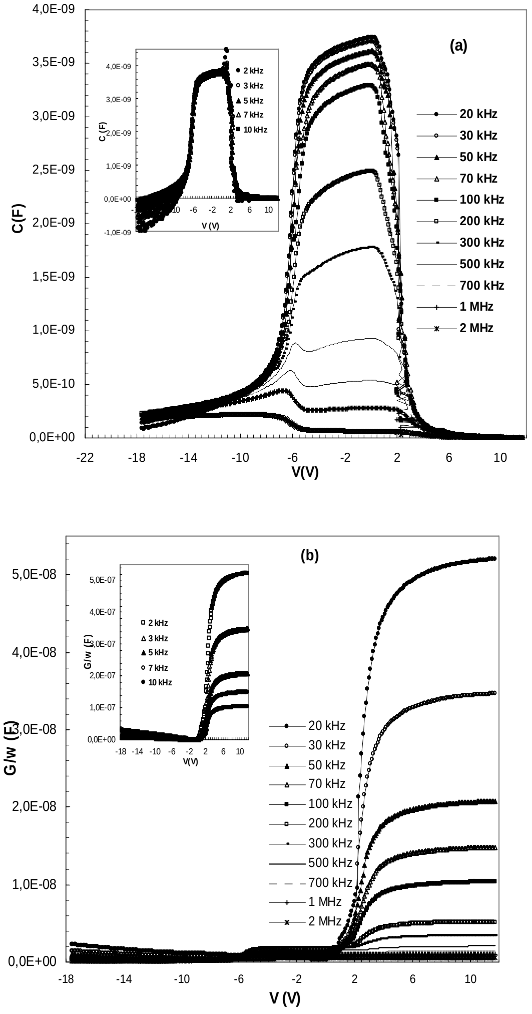

Fig. 3. The frequency dependent curves of (a) the C-V and (b) G/w-V characteristics of (Ni/Au)/AlGaN/AlN/GaN heterostructure at room temperature.

As shown in figures, both the C and G/w decrease with increasing frequency. Because, at low frequencies, the N_{ss} can easily follow the ac signal and yield an excess capacitance, which depends on the frequency and time constant of interface states [1,5,14]. The voltage and frequency dependence R_s was obtained from the measurement capacitance (C_m) and conductance (G_m) at 500, 700 and 1000 kHz [1] and is given in Fig. 4.

$$R_S = \frac{G_{ma}}{G_{ma}^2 + (\omega C_{ma})^2} \tag{5}$$

As shown in Fig. 4, the values of R_s give a peak for each frequency and its magnitude decreases with increasing frequency also the peak position shifts toward the high forward bias region with decreasing frequency. Such behavior of R_s is attributed to interfacial insulator layer (SiN_x) and distribution of N_{ss} at M/S interface.

The density distribution profile of N_{ss} was also obtained from the low-high frequency capacitance measurements as following eq. [1] and is given in Fig. 5.

$$N_{ss} = \frac{q}{A}\left[\left(\frac{1}{C_{LF}} - \frac{1}{C_i}\right)^{-1} - \left(\frac{1}{C_{HF}} - \frac{1}{C_i}\right)^{-1} \right] \tag{6}$$

where C_{LF} and C_{HF} are the measurement low frequency capacitance (5kHz) and high frequency capacitance (1 MHz), respectively, and C_i is the insulator layer capacitance. As shown in Fig 5, the N_{ss} gives a peak and range from $2.7\text{x}10^{11}$ to $1.95\text{x}10^{13}$ $eV^{-1}cm^{-2}$. In addition, the C^{-2}-V plot at 2 MHz shows a linear behavior, indicates that the N_{ss} can not follow the ac signal at this high frequency and consequently do not contribute to appreciably to the structure capacitance.

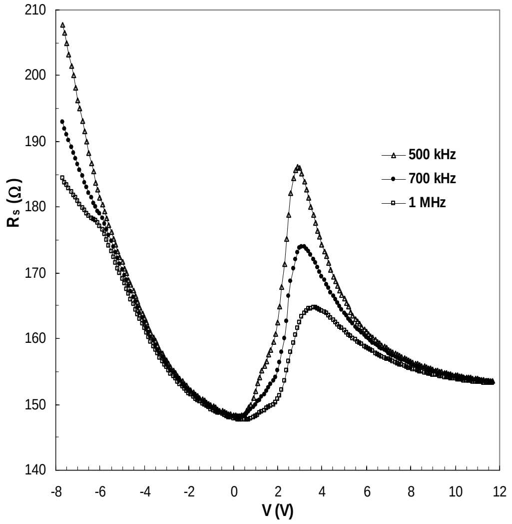

Fig. 4. The R_s versus V plots for (Ni/Au)/AlGaN/AlN/GaN heterostructure.

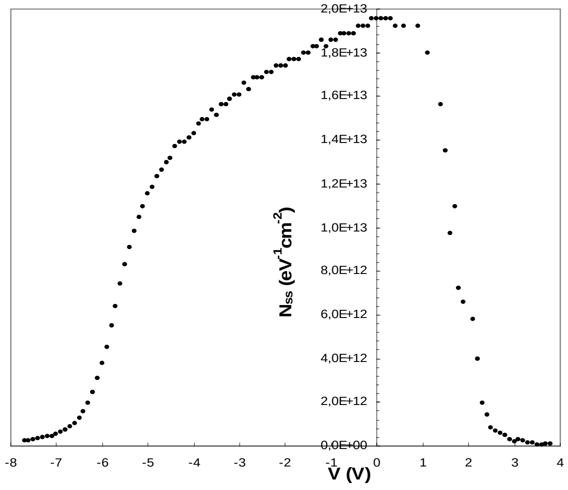

Fig. 5. The N_{ss} profile deduced from the low-high frequency C-V data for heterostructure.

The N_D, W_D, Φ_B and N_{ss} values were obtained from the reverse bias C^{-2}- V plots (Fig. 6) as following equations [10].

$$\Phi_B(C-V) = V_0 + \frac{kT}{q} + E_F \tag{7}$$

where V_0 is the intercept voltage and E_F values were obtained according to,

$$E_F = \frac{kT}{q}\ln\left(\frac{N_C}{N_D}\right) \quad \text{with}$$

$$N_C = 4.82\times10^{15}T^{3/2}\left(\frac{m_e^*}{m_0}\right)^{3/2} \tag{8}$$

where N_C is the effective density of states in conductance band for AlGaN (=$3.03\text{x}10^{18}$ cm^{-3}) and $m_0 = 9.1\times10^{-31}$ kg the rest mass of the electron. The N_D, W_D and Φ_B values were found as $3.30\text{x}10^{17}$ cm^{-3}, $3.97\text{x}10^{-6}$ cm, 0.96 eV, respectively

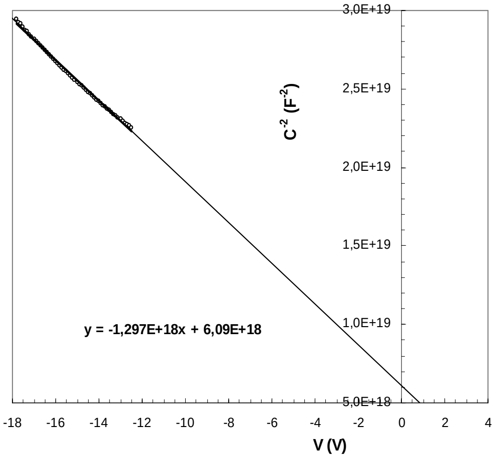

Fig. 6. The C^{-2}-V plot for (Ni/Au)/AlGaN/GaN heterostructure.

4. Conclusions

The (Ni/Au)/AlGaN/AlN/GaN heterostructure with 40 Å interfacial layer (SiN_x) was fabricated in order to investigate the effects of the N_{ss} and R_s on the forward and reverse bias *I-V, C-V,* and *G/w-V* characteristics. The energy density distribution profile of N_{ss} was obtained from the forward bias *I-V* measurements by taking into account the bias dependence of the Φ_e and *n(V)* of the devices and the low-high frequency capacitance methods. The high value of n and R_s were attributed to the existence of an interfacial layer (SiN_x) and N_{ss} at M/S interface. In addition, the voltage dependent R_s profile obtained both I-V and admittance measurements are in good agreement. In conclusion that the existence of interface layer (IL), R_s and N_{ss} lead to deviation from the ideal case of these heterostructures.

References

[1] E. H. Nicollian, J. R. Brews, Metal Oxide Semiconductor (MOS) Physics and Tchnology, John Willey & Sons, New York, 1982.
[2] Ş. Altındal, H.Kanbur, İ. Yücedağ, A. Tataroğlu, Microelectron. Engin. **85**, 1495 (2008).
[3] J. Werner, A. F. J. Levi, R. T. Tung, M. Anzlowar, M. Pinto, Phys. Rev. Lett. **60**, 53 (1988).
[4] P. Chattopadhyay, B. Raychaudhuri, Solid State Electron. **35**, 605 (1993).
[5] S. Zeyrek, Ş. Altındal, H. Yüzer, M. M. Bülbül, Microelectron. Eng. **83**, 577 (2006).
[6] B. R. Chakraborty, N. Dilawar, S. Pal, D. N. Bose, Thin Sol. Films **411**, 240 (2002).
[7] O. Pakma, N. Serin, T. Serin, Ş. Altındal, Semicond. Sci. Technol. **23**, 105014 (2008).
[8] H.C. Card, E.H. Rhoderick. J Phys D: Appl Phys. **4**, 1589 (1971).
[9] R. Castagne, A. Vapaille, Surface Science **28**(1), 157 (1971).
[10] M. Kuhn, Solid State Electron. **13**(6), 873 (1970).
[11] E. Arslan, Ş.Altındal, S. Özçelik, E. Özbay, J. Appl. Phys. **105**, 023705 (2009).
[12] S. M. Sze, Physics Semiconductor Devices, John Wiley and Sons, New York, 1981.
[13] J. P. Sullivan, R. T. Tung, M. R. Pinto, W. R. Graham, J. Appl. Phys. **70**, 7403 (1991).
[14] O. Pakma, N. Serin, T. Serin, Ş. Altındal, J. Phys.D: Appl. Phys. **41**, 215103 (2008).

---

[*] Corresponding author: ilketascioglu@gazi.edu.tr